

S1-26

12728

P-18

N91-28335

I. IDENTIFICATION OF STRENGTHENING PHASES IN  
Al-Cu-Li ALLOY WELDALITE™ 049

IDENTIFICATION OF STRENGTHENING PHASES IN Al-Cu-Li ALLOY  
WELDALITE™ 049†

Microstructure-property relationships were determined for a family of ultrahigh-strength weldable Al-Cu-Li based alloys, developed at Martin Marietta and referred to as Weldalite™ alloys. The highest strength variant of this family, Weldalite™ 049, has a high Cu/Li wt% ratio with a nominal composition of Al-6.3Cu-1.3Li-0.4Ag-0.4Mg-0.14Zr.

Increasing the alloy's lithium content above 1.3 wt% resulted in a decrease in both yield and ultimate tensile strength. Strength was shown to be strongly dependent on lithium content, with a maximum in strength occurring in the range of about 1.1 to 1.4 wt% lithium. The strengthening phases present in Weldalite™ 049 (1.3Li) and an Al-6.3Cu-1.9Li-0.4Ag-0.4Mg-0.14Zr alloy were identified using transmission electron microscopy (TEM).

†Weldalite™ 049 alloys were developed by Martin Marietta Corporation and are used under license from Comalco Aluminum, Ltd.

## INTRODUCTION

Weldalite™ 049, a weldable Al-Cu-Li alloy, obtains ultrahigh strength in the T8 temper. The alloy design considerations and resulting properties are discussed by Pickens et al. (1).

The microstructure of Al-Cu-Li alloys was first studied extensively by Hardy and Silcock (2) and then by Silcock (3), who investigated precipitation after artificial aging (3). Work on the recently commercialized Al-Cu-Li alloy 2090 by Rioja and Ludwiczak (4) and Huang and Ardell (5) confirmed the results of Silcock (3), which show that Al-Cu-Li alloys are strengthened primarily by precipitation of  $T_1$  ( $Al_2CuLi$ ) and/or  $\delta'$  ( $Al_3Li$ ) phases. Both Silcock (3) and Rioja and Ludwiczak (4) showed that the metastable  $\delta'$ -phase was not present if the alloy contained primary  $T_B(Al_{7.5}Cu_4Li)$  phase.

Although Weldalite™ 049 is an Al-Cu-Li based alloy, the relatively minor additions of Mg and Ag give it unique properties. Trace addition effects on precipitation in aluminum alloys have been studied extensively by Polmear and coworkers (6-8) with particular emphasis on Mg and Ag additions. They observed a large increase in strength on adding Mg and Ag to an Al-Cu alloy, resulting from precipitation of the so-called  $\Omega$ -phase with a {111} habit plane, rather than  $\theta^*$ -type† precipitates with a {100} habit plane. The structure of the  $\Omega$ -phase (9) is very close to that of the  $T_1$ -phase, which has been shown to be a very potent strengthener in Al-Cu-Li alloys (10,11).

†  $\theta^*$  represents metastable  $Al_2Cu$  precipitates with a {100} habit plane, e.g.,  $\theta''$ .

In the work reported here, we assessed the tensile properties in the peak-strength T8 temper for Weldalite™ 049 with a Li content ranging from 0 to 1.9 wt% and identified strengthening precipitates at selected Li levels.

### Materials and Experimental Procedures

Weldalite™ 049††-type alloys with lithium contents ranging from 0-1.9††† wt% were fabricated for evaluation. The compositions are given in Table 1.

Table 1

Chemical composition of Weldalite™ 049 variants with different lithium levels as measured using the inductively coupled plasma technique.

Alloy	wt%				
	Cu	Li	Mg	Ag	Zr
049(0)	6.16	---	0.42	0.41	0.14
049(0.9)	5.82	0.88	0.35	0.39	0.16
049(1.3)	5.85	1.25	0.43	0.38	0.13
049(1.6)	6.29	1.62	0.49	0.41	0.16
049(1.9)	6.32	1.86	0.46	0.41	0.14
2090	2.60	2.20	---	---	0.12

†† Hereafter called 049(wt% Li), e.g., 049(1.3), meaning Weldalite™ 049 with a nominal 1.3 wt% Li content.

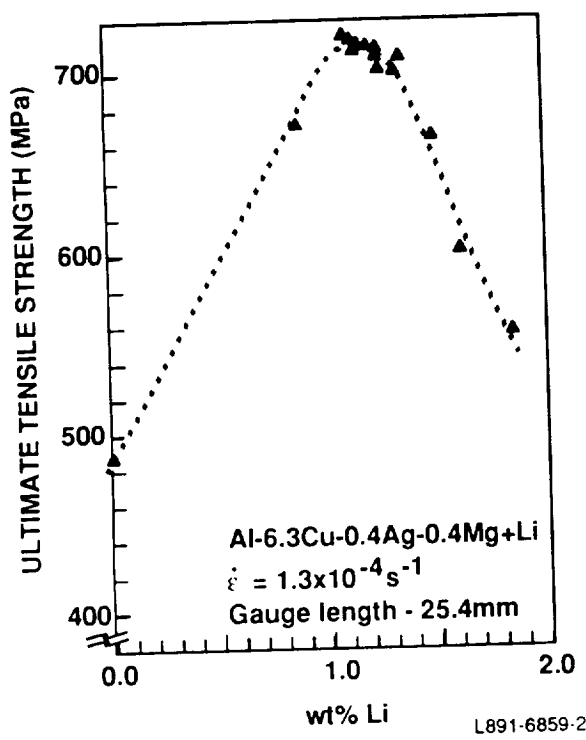
††† Strictly speaking, 049(0) is not a Weldalite™ 049 alloy variant, but since its Cu, Mg, Ag and Zr levels are nominally the same as those in Weldalite™ 049, it will be referred to as 049(0) in this paper. (This alloy is similar to those studied by Polmear.)

Billets weighing 23 kg (50 lb) were cast for each composition using an Ajax vacuum furnace under an Ar cover. The billets were extruded into 9.5-mm x 102-mm (0.375 x 4-in) bar at International Light Metals. Alloys 049(0), 049(0.9), and 049(1.3) were solution heat treated for 1 h at 504°C (940°F), water quenched, and stretched 3.5%; alloys 049(1.6) and 049(1.9) were solution heat treated for 1 h at 493°C (920°F), water quenched, and stretched 3%. Rockwell B hardness ( $R_B$ ) was measured after various times at 160°C (320°F) to determine peak aging conditions for 049(1.3), 049(1.6), and 049(1.9). Peak aging times of 24 h for 049(1.3) and 34 h for 049(1.6) and 049(1.9) were selected based on hardness data. Alloy 2090 T8E41 was used for comparison in certain cases.

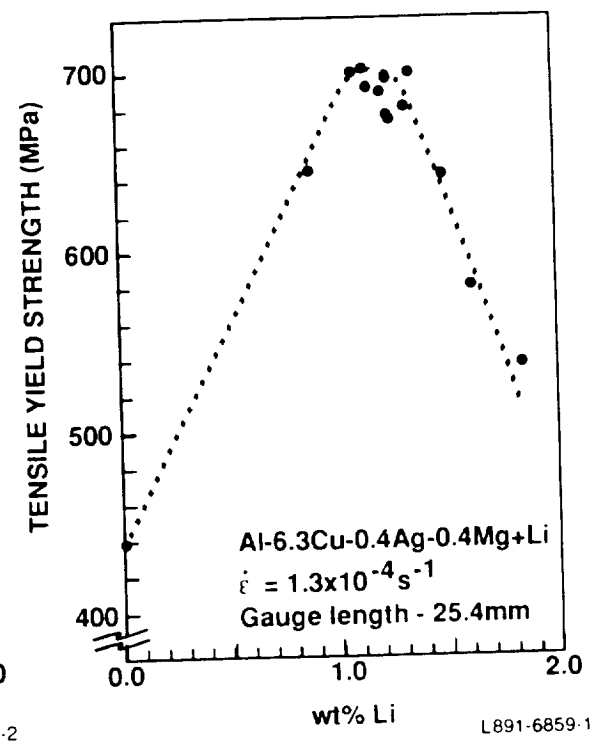
Specimens of selected alloys were examined by transmission electron microscopy (TEM) in a JEOL 100CX at Martin Marietta Laboratories, and by high-resolution TEM (HRTEM) in a Phillips EM430 at the National Institute of Science and Technology in Gaithersburg, MD. Foils were made by jet thinning at -30°C and 11 V in a solution of 75% methanol and 25% nitric acid.

## RESULTS

As previously shown (12), Weldalite™ 049 exhibits a strong strength dependence on lithium content (Fig. 1). Note the peak in both ultimate tensile strength (Fig. 1a) and yield strength (Fig. 1b) at lithium levels between 1.0 and 1.4 wt%. The tensile properties for the variants discussed in this paper are given in Table 2.



(a)



(b)

Figure 1. Ultimate tensile strength (a) and yield strength (b) vs. wt% lithium (Ref. 12).

Table 2

Tensile properties for Weldalite™ 049 with four  
different lithium levels in the T8 temper.

Alloy ID#	Lithium	Aging	Yield	Ultimate	Elongation %
	Content wt%	Time h at 160°C	Strength MPa	Tensile Strength MPa	
049(0)	0.00	24	441	489	12.9
049(1.3)	1.25	24	676	707	3.7
049(1.6)	1.62	34	581	602	5.2
049(1.9)	1.86	34	538	556	3.9

Although a detailed aging study was not performed for 049(0) and 049(0.9), near-peak-aged tensile properties are reported. The data in Fig. 1 and Table 2 clearly indicate that lithium level strongly influences mechanical properties, implying changes in microstructure between 0 and 1.9 wt% lithium. When the compositions of the Weldalite™ 049 variants are plotted on a modified version of Silcock's (3) phase diagram, they fall into four different equilibrium phase fields (Fig. 2). Alloy 049(0) is in an equilibrium two-phase region containing  $Al_{SS}+\theta$ , and should be strengthened by  $\theta^*$ -type precipitates after artificial aging (3). Alloy 049(0.9) is in an equilibrium two-phase field containing  $Al_{SS}+T_B$ . Ternary Al-Cu-Li alloys of this composition were shown by Silcock (3) to be strengthened by  $\theta'$  after artificial aging. Alloy 049(1.3) falls on the boundary of an equilibrium three-phase field with  $Al_{SS}+T_B+T_1$ , and both 049(1.6) and 049(1.9) fall into an equilibrium two-phase field containing  $Al_{SS}+T_1$ . Based on their compositions, and Silcock's work, 049(1.3) should be out of, and 049(1.6) and 049(1.9) should be in the metastable  $\delta'$ -phase field (3,4).

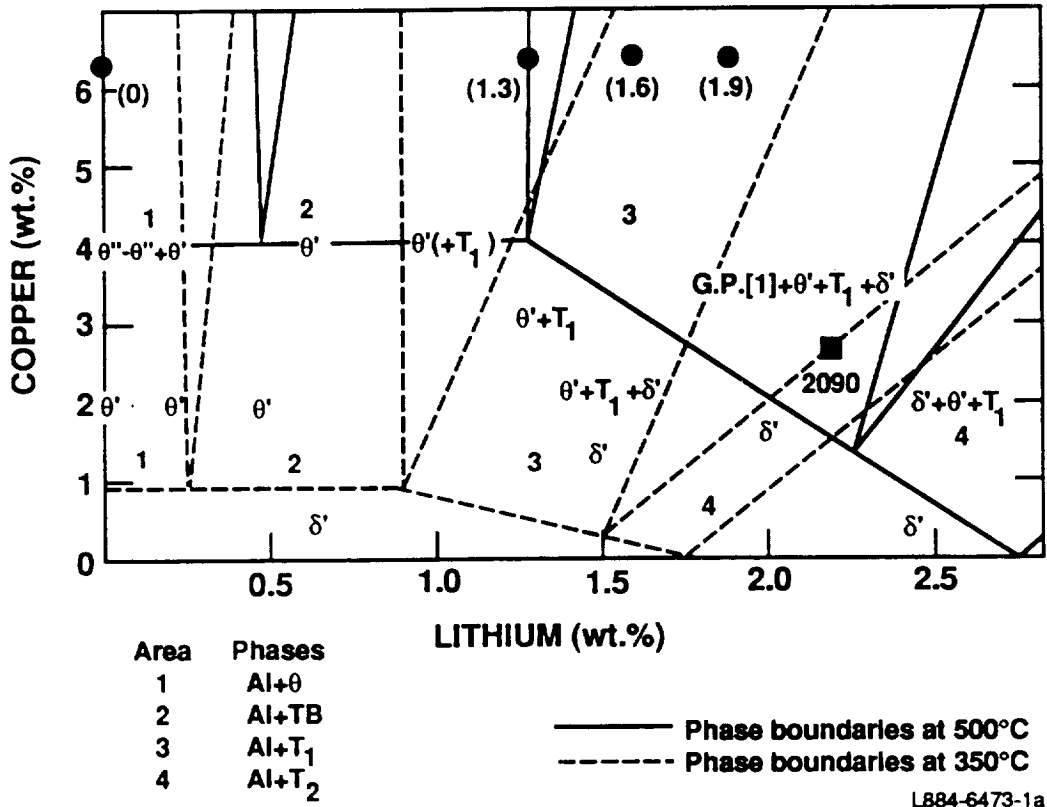


Figure 2. Aluminum corner of the Al-Cu-Li phase diagram (2) with compositions of various Weldalite™ heats. Numbers 1-4 give equilibrium phase relations. Phases observed by Silcock (3), e.g.,  $\theta' + T_1 + \delta'$ , after aging 16 h at 160°C are also shown.

TEM was performed on 049(0), 049(1.3), and 049(1.9) to compare the strengthening phases present in the peak-aged tempers with those observed by Silcock (3) for Al-Cu-Li ternary alloys aged 16 h at 165°C. TEM was also performed on alloy 2090 in the T8E41 temper for comparison purposes. Selected-area electron diffraction (SAD) patterns were indexed for these four alloys with the electron beam direction (B) parallel to the aluminum [112] zone axis (Fig. 3). Reflections from the  $\delta'$ -phase in 2090 appear in Fig. 3d as the bright spots in the superlattice position (indicated by the arrow), and the diffraction from  $T_1$  appears as streaks due to its platelike morphology. The streaking in 049(0) (Fig. 3a) results from diffraction by  $\Omega$  platelets. This streaking coincides with the streaking observed in diffraction from the  $T_1$ -phase, but cannot be  $T_1$  ( $Al_2CuLi$ ) since this alloy has no lithium. The SAD pattern for 049(1.3) (Fig. 3c) with  $B=[112]$  shows streaking similar to that for 2090 and 049(0), indicating that 049(1.3) is strengthened by one of the platelike precipitates with a {111} habit plane, i.e., either  $T_1$  or  $\Omega$ . The  $\delta'$ -phase reflections are not present for this alloy. The SAD pattern with  $B=[112]$  for alloy 049(1.9) (Fig. 3b) shows  $\delta'$  reflections and streaking, indicating that both  $\delta'$  and  $T_1$ -type precipitates are present.

A comparison of the SAD patterns for 049(1.3) and 049(1.9) with  $B=[110]$  confirms the presence of  $\delta'$  in 049(1.9) (Fig. 4). Streaking in the  $\langle 100 \rangle$  direction, due to precipitation on the {100}, is observed in the SAD pattern for 049(1.9) (Fig. 4c), but not in 049(1.3) (Fig. 4a). A dark-field image (DF) from alloy 049(1.3) with  $g=[100]$  and B close to [110] (Fig. 4b) shows only the very faint outline of  $T_1$ -type platelets probably due to streaking from a higher order Laue zone. The DF image for alloy 049(1.9) under similar

ORIGINAL PAGE  
BLACK AND WHITE PHOTOGRAPH

**B = [112]**

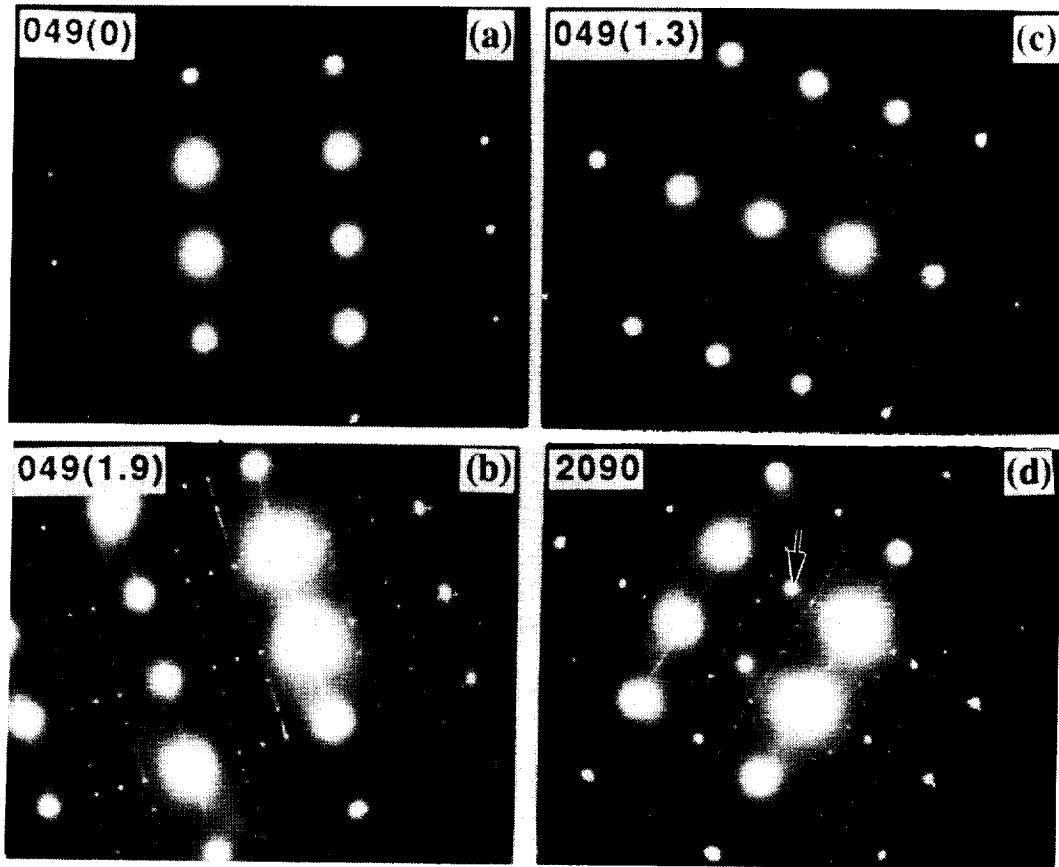


Figure 3. SAD patterns with  $B=[112]$  for (a) 2090, (b) 049(0), (c) 049(1.3), and (d) 049(1.9) in the T8 temper.

ORIGINAL PAGE  
BLACK AND WHITE PHOTOGRAPH

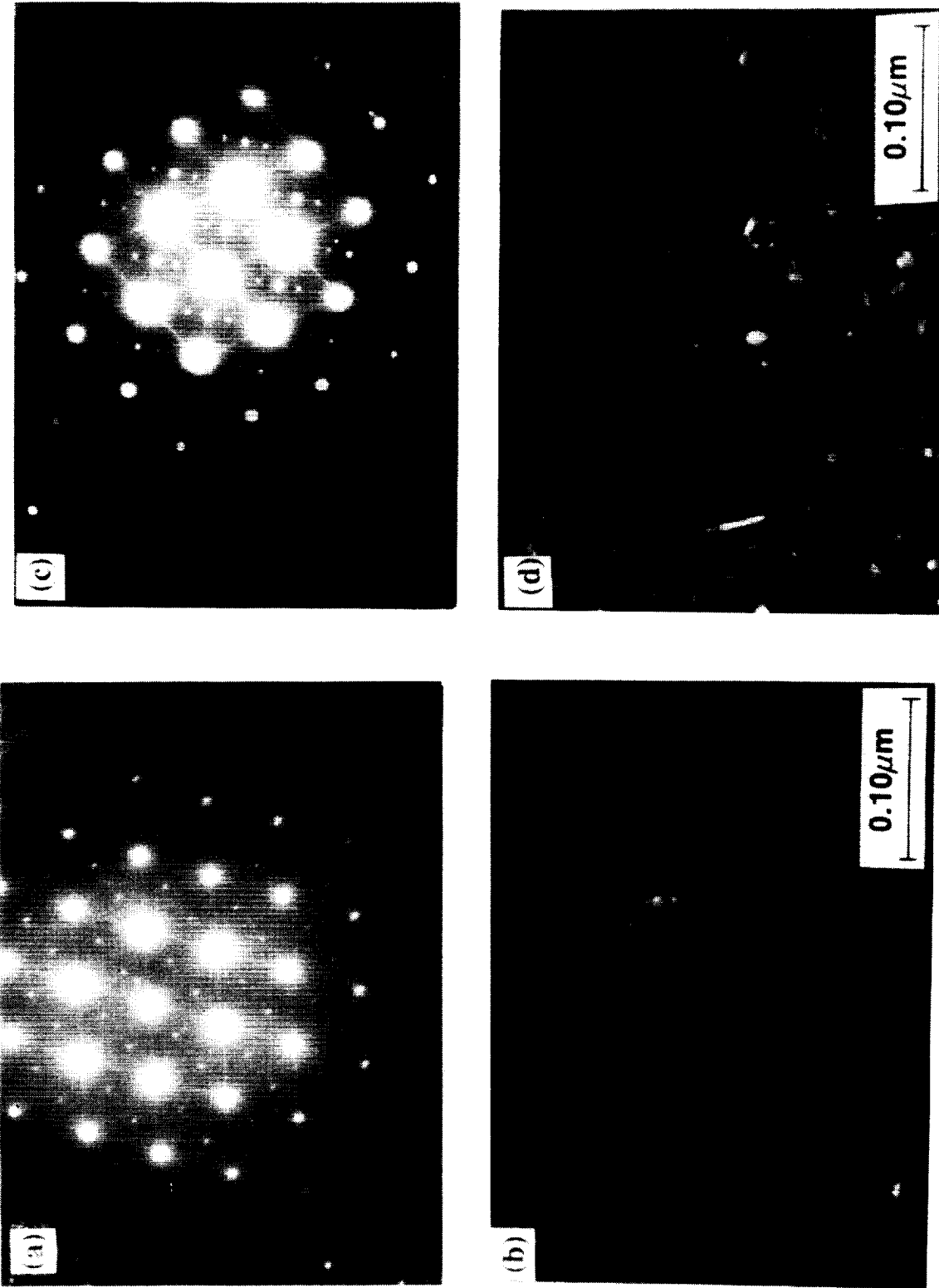


Figure 4. SAD patterns with  $B=[110]$  for (a)  $049(1.3)$  and (c)  $049(1.9)$ ;  $11\bar{1}$  images with  $g=[100]$  for (b)  $049(1.3)$  and (d)  $049(1.9)$ .

diffraction conditions shows the  $\delta'$  and  $\beta'$  ( $\text{Al}_3\text{Zr}/\text{Al}_3\text{Li}$  composite) precipitates and a  $\theta^*$ -type precipitate (Fig. 4d).

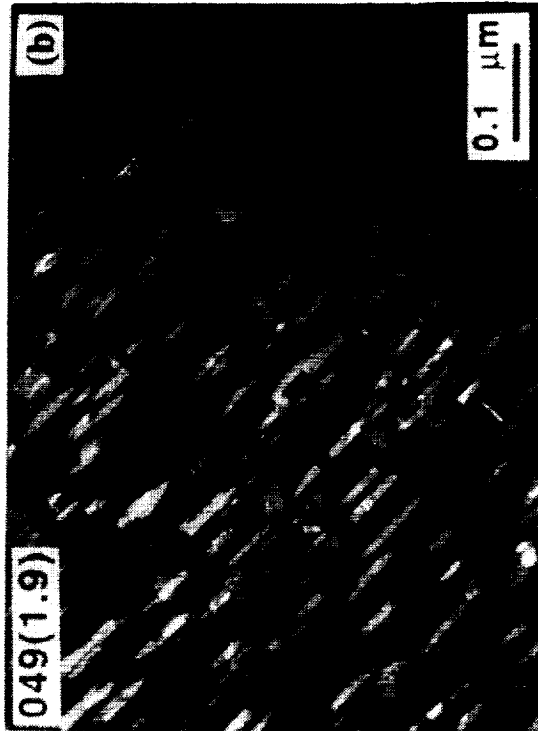
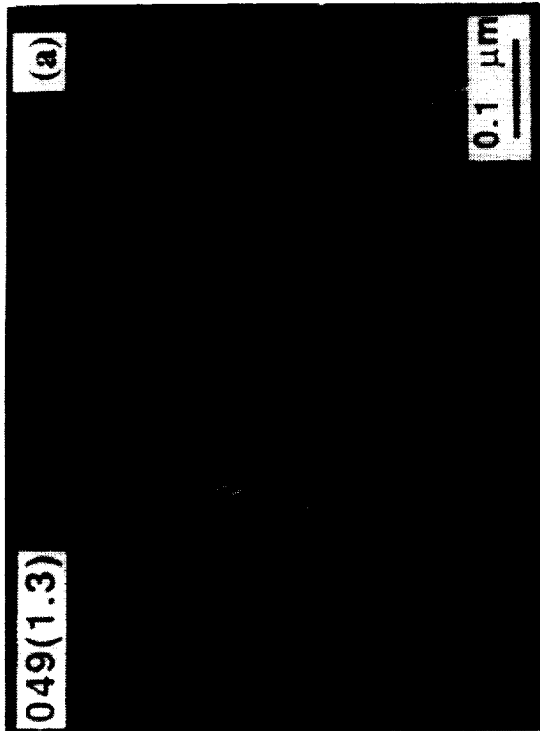
Dark-field micrographs for alloys 049(1.3) and 049(1.9), with  $g=[2020]$  and  $B$  close to the  $[110]$  and  $[111]$  zone axis, show that the precipitates are regularly shaped (Fig. 5). Huang and Ardell (5) give details of the spatial relationships between the inclined  $T_1$  platelets for alloy 2090, and these relationships should remain unchanged for the platelets in the Weldalite™ 049 alloy regardless of whether they are  $\Omega$  or  $T_1$ . Although neither the volume nor number fraction can be assessed from this limited number of micrographs, qualitatively, the  $T_1$  size and morphology appear similar for the two Weldalite™ alloys.

Based on preliminary HRTEM for  $T_1$ -type precipitates in peak-aged 049(1.3), the precipitates are  $\sim 10$  Å thick and have a stacking sequence similar to that of the  $T_1$  precipitates imaged by Cassada et al. (13) (Fig. 6; note insert). Growth ledges are observed, but, based on the proposed stacking sequence for  $T_1$ , all precipitates imaged are essentially one unit cell thick.

## DISCUSSION

We propose that the sharp decrease in strength associated with increasing lithium content from 1.3 to 1.9 wt% is associated with the precipitation of  $\delta'$  at the expense of  $T_1$ . A qualitative comparison of the  $T_1$  precipitates in 049(1.3) and 049(1.9) (Fig. 5) indicates that the precipitation of the  $\delta'$ -phase in 049(1.9) does not change the  $T_1$  precipitate size. Consequently, the variation in strength between 049(1.3) and 049(1.9) is not related to a change in the  $T_1$  platelet size.

$B = [111]$



$B = [110]$

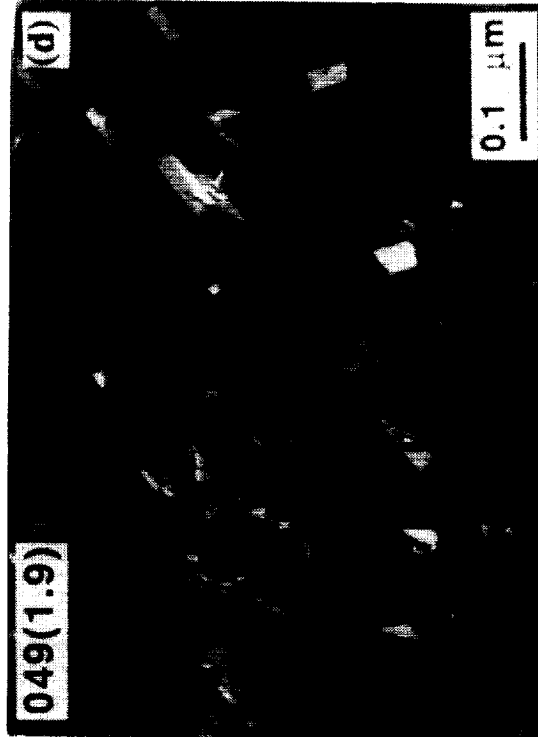
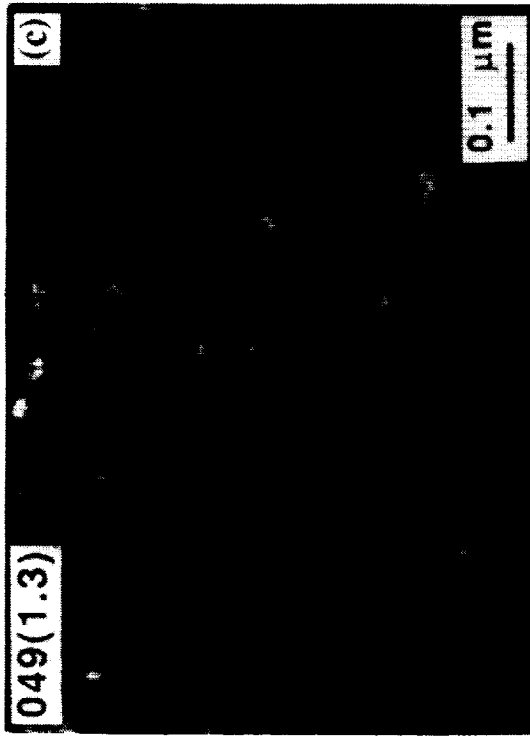


Figure 5. DF images for (a) 049(1.3) and (b) 049(1.9) with  $g = [2020]$ ,  $B = [110]$ ; for (c) 049(1.3) and (d) 049(1.9) with  $g = [2020]$ ,  $B = [111]$ .

ORIGINAL PAGE  
BLACK AND WHITE PHOTOGRAPH

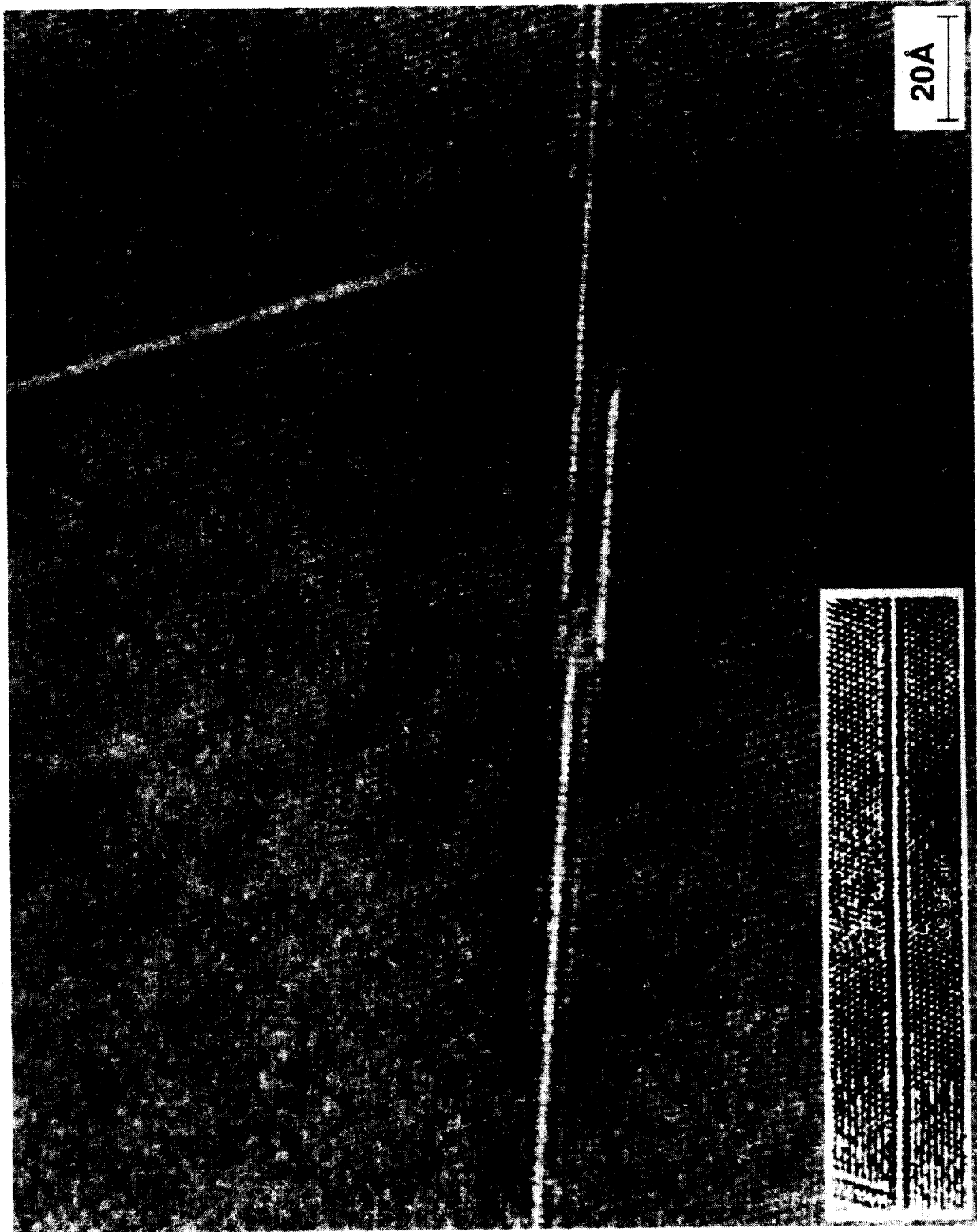


Figure 6. HRTEM for 049(1.3) with  $B=[111]$ ; insert from Ref. 13.

Huang and Ardell (10,11,14) showed that the  $T_1$ -phase is a more potent strengthener than the  $\delta'$ -phase in Al-Cu-Li alloys, and that the strength contribution from the  $T_1$ -phase ( $\Delta\tau_{T_1}$ ) and  $\delta'$ -phase ( $\Delta\tau_{\delta'}$ ) to the critically resolved shear stress (CRSS) ( $\Delta\tau_\rho$ ) of an alloy follows a generalized superposition rule:

$$\Delta\tau_\rho^q = \Delta\tau_{T_1}^q + \Delta\tau_{\delta'}^q \quad (1)$$

where  $q$  is between 1 and 2.

Thus, if the  $T_1$  distribution and size were to remain constant in the peak-aged temper for alloys 049(1.3) and 049(1.9), then the addition of the  $\delta'$ -phase would increase strength. The precipitation of  $\delta'$  in the Weldalite™ 049 variants resulted in a strength decrease, so if this superposition rule is obeyed and solid-solution strengthening effects are small, then the precipitation of  $\delta'$  would occur at the expense of the  $T_1$ -phase. Although we need to obtain supporting quantitative data, based on these assumptions, it appears that precipitation of the  $\delta'$ -phase must result in a decrease in volume fraction of the  $T_1$ -phase.

No  $\theta^*$ -type precipitates were present in 049(0) or 049(1.3), which is contrary to the results of Silcock (3) for ternary alloys with similar compositions. Both alloys have a uniform distribution of very thin, coherent, platelike precipitates with a  $\{111\}$  habit plane. The  $T_1$ -phase in 2090 and the  $\omega$ -phase in Al-Cu-Mg-Ag alloys are both hexagonal (9) and have platelike morphology with a  $\{111\}$  habit plane. Kerry and Scott (9) determined lattice parameters of  $a=0.496$  nm and  $c/a=1.414$  for the  $\omega$ -phase, which are similar to the cell dimensions for  $T_1$  ( $Al_2CuLi$ ) found by Hardy and Silcock (2), i.e.,

$a=0.496$  nm and  $c=0.935$  nm ( $c/a=1.885$ ). Although the stoichiometry of the  $\Omega$ -phase is unknown, it is believed to be an  $Al_2Cu$ -type precipitate. Both  $\Omega$  and  $T_1$  precipitates have the same crystallographic relationship with the matrix --  $(111)_{Al} \parallel (0001)_{\text{precipitate}}$  -- and a  $c$ -axis perpendicular to the face of the platelet. The plate dimensions parallel to the  $c$ -axis are very thin. As a result, diffraction from these platelets produces extensive streaking in the reciprocal lattice, which obscures the structure. This streaking, in combination with the identical lengths of the unit cell dimension " $a$ ," make it extremely difficult to differentiate  $T_1$  from  $\Omega$  in the peak-aged temper. Detailed HRTEM is under way to determine if Weldalite™ 049 is strengthened by  $T_1$ ,  $\Omega$ , or both phases in the peak-aged temper.

Polmear and coworkers (6-8) and Kerry and Scott (9), showed that Mg and Ag additions stimulate precipitation on the  $\{111\}$  in Al-Cu alloys. Scott et al. (6) proposed that precipitation is stimulated by changing the vacancy-solute interactions and the alloys' stacking fault energy (15). It is also possible that similar mechanisms apply in Weldalite™ 049.

### CONCLUSIONS

1. Relatively small amounts of Ag and Mg are extremely effective in stimulating precipitation in Al-6.3Cu-1.3Li-0.4Ag-0.4Mg-0.14Zr alloy, Weldalite™ 049, resulting in a homogeneous distribution of fine, platelike precipitates with a  $\{111\}$  habit plane in the peak-aged, T8 temper.

2. The yield and tensile strengths are strongly dependent on Li content, with a peak in the range of 1.1 to 1.4 wt% Li. At >1.4 wt% Li, strength decreases rapidly, which is associated with  $\delta'$  precipitation.
3. From HRTEM, the structure of  $T_1$ -type precipitates in Weldalite™ 049 is similar to that of  $T_1$  platelets in 2090.

#### ACKNOWLEDGEMENTS

This work was supported by NASA Contract #NASI-18531, and the authors wish to thank Bill Brewer, Contract Monitor, for his support. We are especially grateful to Dr. F.H. Heubaum for generating some of the mechanical property data on the Weldalite™ alloys. We would also like to thank Drs. F.H. Heubaum, F.W. Gayle, and A.J. Ardell for their enlightening discussions.

#### REFERENCES

- (1) Pickens, J.R., Heubaum, F.H., Langan, T.J., and Kramer, L.S., Proc. of Fifth Int. Conf. on Al-Li Alloys, Williamsburg, Virginia, 1989.
- (2) Hardy, H.K. and Silcock, J.M., J. Inst. Metals, Vol. 84, 1955-56, pp. 423-428.
- (3) Silcock, J.M., J. Inst. Metals, Vol. 88, 1959-60, pp. 357-364.
- (4) Rioja, R.J. and Ludwiczak, E.A., "Aluminum-Lithium Alloys III," Edited by C. Baker et al., Inst. of Metals, London, 1986, pp. 471-482.

- (5) Huang, J.C. and Ardell, A.J., *Mat. Sci. and Tech.*, Vol. 3, 1987, pp. 176-188.
- (6) Chester, R.J. and Polmear, I.J., "The Metallurgy of Light Alloys," *Inst. of Metallurgists, London*, 1983, pp. 75-81.
- (7) Polmear, I.J. and Couper, M.J., *Met. Trans.*, Vol. 19A, 1988, pp. 1027-1035.
- (8) Vietz, J.T. and Polmear, I.J., *J. Inst. Metals*, Vol. 94, 1966, pp. 410-419.
- (9) Kerry, S. and Scott, V.D., *Met. Sci.*, Vol. 18, 1984, pp. 289-294.
- (10) Huang, J.C. and Ardell, A.J., *Acta Met.*, Vol. 36, 1988, pp. 2995-3006.
- (11) Huang, J.C. and Ardell, A.J., "4th International Aluminum-Lithium Conf.," Edited by G. Champier et al., pp. C3-373-396; *J. Phys.*, 48, Colleague C3, Suppl. 9, Les Editions de Physique, Les Ulis, France, 1987.
- (12) J.R. Pickens, F.H. Heubaum, L.S. Kramer, and K.S. Kumar, U.S. Patent Application Serial No. 07/327,927 Filed March 23, 1989 which is a Continuation-in-Part (CIP) of Serial No. 083,333 Filed August 10, 1987.
- (13) Cassada, W.A., Shiflet, G.J., and Starke, E.A., *ibid.* Ref. 11, pp. C3-397-406.
- (14) Huang, J.C. and Ardell, A.J., "Aluminium Technology '86," Edited by T. Sheppard, *Inst. of Metals, London*, 1986, pp. 434-441.
- (15) Scott, V.D., Kerry, S., and Trumper, R.L., *Met. Sci. and Tech.*, Vol. 3, 1987, pp. 827-834.